

Observation of  $B^+ \rightarrow \chi_{c0} K^+$ 

The Belle Collaboration

## Abstract

We report the first observation of the decay  $B^+ \rightarrow \chi_{c0} K^+$  using  $21.3 \text{ fb}^{-1}$  of data collected by the Belle detector at the  $\Upsilon(4S)$  resonance. The preliminary result for the branching fraction is  $\mathcal{B}(B^+ \rightarrow \chi_{c0} K^+) = (8.0_{-2.4}^{+2.7} \pm 1.0 \pm 1.1) \times 10^{-4}$  where the first error is statistical, the second is systematic, and the third comes from the uncertainty in the  $\chi_{c0} \rightarrow \pi^+ \pi^-$  branching fraction.

K. Abe<sup>9</sup>, K. Abe<sup>37</sup>, R. Abe<sup>27</sup>, I. Adachi<sup>9</sup>, Byoung Sup Ahn<sup>16</sup>, H. Aihara<sup>39</sup>, M. Akatsu<sup>20</sup>,  
 K. Asai<sup>21</sup>, M. Asai<sup>10</sup>, Y. Asano<sup>44</sup>, T. Aso<sup>43</sup>, V. Aulchenko<sup>2</sup>, T. Aushev<sup>14</sup>, A. M. Bakich<sup>35</sup>,  
 E. Banas<sup>25</sup>, S. Behari<sup>9</sup>, P. K. Behera<sup>45</sup>, D. Beilne<sup>2</sup>, A. Bondar<sup>2</sup>, A. Bozek<sup>25</sup>,  
 T. E. Browder<sup>8</sup>, B. C. K. Casey<sup>8</sup>, P. Chang<sup>24</sup>, Y. Chao<sup>24</sup>, K.-F. Chen<sup>24</sup>, B. G. Cheon<sup>34</sup>,  
 R. Chistov<sup>14</sup>, S.-K. Choi<sup>7</sup>, Y. Choi<sup>34</sup>, L. Y. Dong<sup>12</sup>, J. Dragic<sup>19</sup>, A. Drutskoy<sup>14</sup>,  
 S. Eidelman<sup>2</sup>, V. Eiges<sup>14</sup>, Y. Enari<sup>20</sup>, C. W. Everton<sup>19</sup>, F. Fang<sup>8</sup>, H. Fujii<sup>9</sup>, C. Fukunaga<sup>41</sup>,  
 M. Fukushima<sup>11</sup>, N. Gabyshev<sup>9</sup>, A. Garmash<sup>2,9</sup>, T. J. Gershon<sup>9</sup>, A. Gordon<sup>19</sup>, K. Gotow<sup>46</sup>,  
 H. Guler<sup>8</sup>, R. Guo<sup>22</sup>, J. Haba<sup>9</sup>, H. Hamasaki<sup>9</sup>, K. Hanagaki<sup>31</sup>, F. Handa<sup>38</sup>, K. Hara<sup>29</sup>,  
 T. Hara<sup>29</sup>, N. C. Hastings<sup>19</sup>, H. Hayashii<sup>21</sup>, M. Hazumi<sup>29</sup>, E. M. Heenan<sup>19</sup>, Y. Higashino<sup>20</sup>,  
 I. Higuchi<sup>38</sup>, T. Higuchi<sup>39</sup>, T. Hirai<sup>40</sup>, H. Hirano<sup>42</sup>, T. Hojo<sup>29</sup>, T. Hokuue<sup>20</sup>, Y. Hoshi<sup>37</sup>,  
 K. Hoshina<sup>42</sup>, S. R. Hou<sup>24</sup>, W.-S. Hou<sup>24</sup>, S.-C. Hsu<sup>24</sup>, H.-C. Huang<sup>24</sup>, Y. Igarashi<sup>9</sup>,  
 T. Iijima<sup>9</sup>, H. Ikeda<sup>9</sup>, K. Ikeda<sup>21</sup>, K. Inami<sup>20</sup>, A. Ishikawa<sup>20</sup>, H. Ishino<sup>40</sup>, R. Itoh<sup>9</sup>,  
 G. Iwai<sup>27</sup>, H. Iwasaki<sup>9</sup>, Y. Iwasaki<sup>9</sup>, D. J. Jackson<sup>29</sup>, P. Jalocha<sup>25</sup>, H. K. Jang<sup>33</sup>, M. Jones<sup>8</sup>,  
 R. Kagan<sup>14</sup>, H. Kakuno<sup>40</sup>, J. Kaneko<sup>40</sup>, J. H. Kang<sup>48</sup>, J. S. Kang<sup>16</sup>, P. Kapusta<sup>25</sup>,  
 N. Katayama<sup>9</sup>, H. Kawai<sup>3</sup>, H. Kawai<sup>39</sup>, Y. Kawakami<sup>20</sup>, N. Kawamura<sup>1</sup>, T. Kawasaki<sup>27</sup>,  
 H. Kichimi<sup>9</sup>, D. W. Kim<sup>34</sup>, Heejong Kim<sup>48</sup>, H. J. Kim<sup>48</sup>, Hyunwoo Kim<sup>16</sup>, S. K. Kim<sup>33</sup>,  
 T. H. Kim<sup>48</sup>, K. Kinoshita<sup>5</sup>, S. Kobayashi<sup>32</sup>, S. Koishi<sup>40</sup>, H. Konishi<sup>42</sup>, K. Korotushenko<sup>31</sup>,  
 P. Krokovny<sup>2</sup>, R. Kulasiri<sup>5</sup>, S. Kumar<sup>30</sup>, T. Kuniya<sup>32</sup>, E. Kurihara<sup>3</sup>, A. Kuzmin<sup>2</sup>,  
 Y.-J. Kwon<sup>48</sup>, J. S. Lange<sup>6</sup>, G. Leder<sup>13</sup>, S. H. Lee<sup>33</sup>, C. Leonidopoulos<sup>31</sup>, Y.-S. Lin<sup>24</sup>,  
 D. Liventsev<sup>14</sup>, R.-S. Lu<sup>24</sup>, J. MacNaughton<sup>13</sup>, D. Marlow<sup>31</sup>, T. Matsubara<sup>39</sup>, S. Matsui<sup>20</sup>,  
 S. Matsumoto<sup>4</sup>, T. Matsumoto<sup>20</sup>, Y. Mikami<sup>38</sup>, K. Misono<sup>20</sup>, K. Miyabayashi<sup>21</sup>,  
 H. Miyake<sup>29</sup>, H. Miyata<sup>27</sup>, L. C. Moffitt<sup>19</sup>, G. R. Moloney<sup>19</sup>, G. F. Moorhead<sup>19</sup>, S. Mori<sup>44</sup>,  
 T. Mori<sup>4</sup>, A. Murakami<sup>32</sup>, T. Nagamine<sup>38</sup>, Y. Nagasaka<sup>10</sup>, Y. Nagashima<sup>29</sup>, T. Nakadaira<sup>39</sup>,  
 T. Nakamura<sup>40</sup>, E. Nakano<sup>28</sup>, M. Nakao<sup>9</sup>, H. Nakazawa<sup>4</sup>, J. W. Nam<sup>34</sup>, Z. Natkaniec<sup>25</sup>,  
 K. Neichi<sup>37</sup>, S. Nishida<sup>17</sup>, O. Nitoh<sup>42</sup>, S. Noguchi<sup>21</sup>, T. Nozaki<sup>9</sup>, S. Ogawa<sup>36</sup>, T. Ohshima<sup>20</sup>,  
 Y. Ohshima<sup>40</sup>, T. Okabe<sup>20</sup>, T. Okazaki<sup>21</sup>, S. Okuno<sup>15</sup>, S. L. Olsen<sup>8</sup>, H. Ozaki<sup>9</sup>,  
 P. Pakhlov<sup>14</sup>, H. Palka<sup>25</sup>, C. S. Park<sup>33</sup>, C. W. Park<sup>16</sup>, H. Park<sup>18</sup>, L. S. Peak<sup>35</sup>, M. Peters<sup>8</sup>,  
 L. E. Piilonen<sup>46</sup>, E. Prebys<sup>31</sup>, J. L. Rodriguez<sup>8</sup>, N. Root<sup>2</sup>, M. Rozanska<sup>25</sup>, K. Rybicki<sup>25</sup>,  
 J. Ryuko<sup>29</sup>, H. Sagawa<sup>9</sup>, Y. Sakai<sup>9</sup>, H. Sakamoto<sup>17</sup>, M. Satapathy<sup>45</sup>, A. Satpathy<sup>9,5</sup>,  
 S. Schrenk<sup>5</sup>, S. Semenov<sup>14</sup>, K. Senyo<sup>20</sup>, Y. Settai<sup>4</sup>, M. E. Sevier<sup>19</sup>, H. Shibuya<sup>36</sup>,  
 B. Shwartz<sup>2</sup>, A. Sidorov<sup>2</sup>, S. Stanič<sup>44</sup>, A. Sugi<sup>20</sup>, A. Sugiyama<sup>20</sup>, K. Sumisawa<sup>9</sup>,  
 T. Sumiyoshi<sup>9</sup>, J.-I. Suzuki<sup>9</sup>, K. Suzuki<sup>3</sup>, S. Suzuki<sup>47</sup>, S. Y. Suzuki<sup>9</sup>, S. K. Swain<sup>8</sup>,  
 H. Tajima<sup>39</sup>, T. Takahashi<sup>28</sup>, F. Takasaki<sup>9</sup>, M. Takita<sup>29</sup>, K. Tamai<sup>9</sup>, N. Tamura<sup>27</sup>,  
 J. Tanaka<sup>39</sup>, M. Tanaka<sup>9</sup>, G. N. Taylor<sup>19</sup>, Y. Teramoto<sup>28</sup>, M. Tomoto<sup>9</sup>, T. Tomura<sup>39</sup>,  
 S. N. Tovey<sup>19</sup>, K. Trabelsi<sup>8</sup>, T. Tsuboyama<sup>9</sup>, T. Tsukamoto<sup>9</sup>, S. Uehara<sup>9</sup>, K. Ueno<sup>24</sup>,  
 Y. Unno<sup>3</sup>, S. Uno<sup>9</sup>, Y. Ushiroda<sup>9</sup>, S. E. Vahsen<sup>31</sup>, K. E. Varvell<sup>35</sup>, C. C. Wang<sup>24</sup>,  
 C. H. Wang<sup>23</sup>, J. G. Wang<sup>46</sup>, M.-Z. Wang<sup>24</sup>, Y. Watanabe<sup>40</sup>, E. Won<sup>33</sup>, B. D. Yabsley<sup>9</sup>,  
 Y. Yamada<sup>9</sup>, M. Yamaga<sup>38</sup>, A. Yamaguchi<sup>38</sup>, H. Yamamoto<sup>8</sup>, T. Yamanaka<sup>29</sup>,  
 Y. Yamashita<sup>26</sup>, M. Yamauchi<sup>9</sup>, S. Yanaka<sup>40</sup>, J. Yashima<sup>9</sup>, M. Yokoyama<sup>39</sup>, K. Yoshida<sup>20</sup>,  
 Y. Yusa<sup>38</sup>, H. Yuta<sup>1</sup>, C. C. Zhang<sup>12</sup>, J. Zhang<sup>44</sup>, H. W. Zhao<sup>9</sup>, Y. Zheng<sup>8</sup>, V. Zhilich<sup>2</sup>, and  
 D. Žontar<sup>44</sup>

<sup>1</sup>Aomori University, Aomori

<sup>2</sup>Budker Institute of Nuclear Physics, Novosibirsk

<sup>3</sup>Chiba University, Chiba

<sup>4</sup>Chuo University, Tokyo

- <sup>5</sup>University of Cincinnati, Cincinnati OH
- <sup>6</sup>University of Frankfurt, Frankfurt
- <sup>7</sup>Gyeongsang National University, Chinju
- <sup>8</sup>University of Hawaii, Honolulu HI
- <sup>9</sup>High Energy Accelerator Research Organization (KEK), Tsukuba
- <sup>10</sup>Hiroshima Institute of Technology, Hiroshima
- <sup>11</sup>Institute for Cosmic Ray Research, University of Tokyo, Tokyo
- <sup>12</sup>Institute of High Energy Physics, Chinese Academy of Sciences, Beijing
- <sup>13</sup>Institute of High Energy Physics, Vienna
- <sup>14</sup>Institute for Theoretical and Experimental Physics, Moscow
- <sup>15</sup>Kanagawa University, Yokohama
- <sup>16</sup>Korea University, Seoul
- <sup>17</sup>Kyoto University, Kyoto
- <sup>18</sup>Kyungpook National University, Taegu
- <sup>19</sup>University of Melbourne, Victoria
- <sup>20</sup>Nagoya University, Nagoya
- <sup>21</sup>Nara Women's University, Nara
- <sup>22</sup>National Kaohsiung Normal University, Kaohsiung
- <sup>23</sup>National Lien-Ho Institute of Technology, Miao Li
- <sup>24</sup>National Taiwan University, Taipei
- <sup>25</sup>H. Niewodniczanski Institute of Nuclear Physics, Krakow
- <sup>26</sup>Nihon Dental College, Niigata
- <sup>27</sup>Niigata University, Niigata
- <sup>28</sup>Osaka City University, Osaka
- <sup>29</sup>Osaka University, Osaka
- <sup>30</sup>Panjab University, Chandigarh
- <sup>31</sup>Princeton University, Princeton NJ
- <sup>32</sup>Saga University, Saga
- <sup>33</sup>Seoul National University, Seoul
- <sup>34</sup>Sungkyunkwan University, Suwon
- <sup>35</sup>University of Sydney, Sydney NSW
- <sup>36</sup>Toho University, Funabashi
- <sup>37</sup>Tohoku Gakuin University, Tagajo
- <sup>38</sup>Tohoku University, Sendai
- <sup>39</sup>University of Tokyo, Tokyo
- <sup>40</sup>Tokyo Institute of Technology, Tokyo
- <sup>41</sup>Tokyo Metropolitan University, Tokyo
- <sup>42</sup>Tokyo University of Agriculture and Technology, Tokyo
- <sup>43</sup>Toyama National College of Maritime Technology, Toyama
- <sup>44</sup>University of Tsukuba, Tsukuba
- <sup>45</sup>Utkal University, Bhubaneswer
- <sup>46</sup>Virginia Polytechnic Institute and State University, Blacksburg VA
- <sup>47</sup>Yokkaichi University, Yokkaichi
- <sup>48</sup>Yonsei University, Seoul

## I. INTRODUCTION

The production rate of quarkonium states in various high energy physics processes can provide valuable insight not only into the interactions between a heavy quark and antiquark, but also into the elementary processes with the production of a  $Q\bar{Q}$  pair. The spin-1  $S$ -wave resonances, such as the  $J/\psi$  of the charmonium family, are of special experimental significance because of their importance for studies of  $CP$  violation. The  $P$  states are also important in their own right because they probe a qualitatively different aspect of the  $Q\bar{Q}$  production process. While the  $S$  states probe only the production of color-singlet  $Q\bar{Q}$  pairs at small separation distances, the  $P$  states can also probe the production of color-octet  $Q\bar{Q}$  pairs. Color-singlet production of  $\chi_{c0}$  in  $B$  decays vanishes in the factorization approximation as a consequence of spin-parity conservation. However, the color-octet mechanism allows for the production of the  $\chi_{c0}$   $P$ -wave  $0^{++}$  state via the emission of a soft gluon [1,2].

The only recent search for the  $B \rightarrow \chi_{c0}K$  decay was reported by CLEO [3]. Using  $9.66 \times 10^6$   $B\bar{B}$  pairs they set 90% C.L. upper limits of:  $\mathcal{B}(B^+ \rightarrow \chi_{c0}K^+) < 4.8 \times 10^{-4}$  and  $\mathcal{B}(B^0 \rightarrow \chi_{c0}K^0) < 5.0 \times 10^{-4}$ . This analysis uses a data sample collected with the Belle detector [4] at KEKB asymmetric energy  $e^+e^-$  collider [5]. It consists of  $21.3 \text{ fb}^{-1}$  taken at the  $\Upsilon(4S)$  (which corresponds to about 22.8 million produced  $B\bar{B}$  pairs) and  $2.3 \text{ fb}^{-1}$  taken 60 MeV below for continuum studies.

The detailed analysis of the final state presented in this paper is part of the general analysis of  $B$ -meson three-body decays reported in ref. [6].

The inclusion of charge conjugate states is implicit throughout this report unless explicitly stated otherwise.

## II. EVENT SELECTION

Charged tracks are required to satisfy a set of track quality cuts based on the average hit residual and impact parameters in both  $r$ - $\phi$  and  $r$ - $z$  planes. We require that the transverse momentum of the track be greater than 100 MeV/ $c$  to reduce low momentum combinatorial background. For more details, see ref. [6].

Hadron identification is accomplished using the responses of the ACC and the TOF and  $dE/dx$  measurements in the CDC. The information from these three subsystems is combined in a single number using the likelihood method:

$$\mathcal{L}(h) = \mathcal{L}^{ACC}(h) \times \mathcal{L}^{TOF}(h) \times \mathcal{L}^{CDC}(h),$$

where  $h$  stands for the hadron type ( $\pi, K, p$ ). Charged particles are identified as  $K$ 's or  $\pi$ 's by cutting on the likelihood ratio (PID):

$$PID(K) = \frac{\mathcal{L}(K)}{\mathcal{L}(K) + \mathcal{L}(\pi)}; PID(\pi) = \frac{\mathcal{L}(\pi)}{\mathcal{L}(\pi) + \mathcal{L}(K)} = 1 - PID(K)$$

The likelihood ratio for kaon candidates is required to be greater than 0.5 and for pion candidates less than 0.9.

All charged tracks are also required to satisfy an electron veto requirement that demands that the electron likelihood is less than 0.95. In addition, all charged kaon candidates are required to satisfy a proton veto:

$$PID(p) = \frac{\mathcal{L}(p)}{\mathcal{L}(p) + \mathcal{L}(K)} < 0.95.$$

For more details see ref. [6] and references therein.

We reconstruct  $\chi_{c0}$  candidates in the  $\chi_{c0} \rightarrow \pi^+\pi^-$  and  $\chi_{c0} \rightarrow K^+K^-$  decay modes. The  $B^+ \rightarrow \chi_{c0}K^+$  candidate events are identified by means of the beam-constrained mass  $M_{BC}$  and the energy difference  $\Delta E$ :

$$M_{BC} = \sqrt{s/4 - P_B^{*2}}; \quad \Delta E = E_B^* - \sqrt{s}/2,$$

where  $E_B^*$  and  $P_B^*$  are the energy and three-momentum of the  $B$  candidate in the  $\Upsilon(4S)$  rest frame and  $\sqrt{s}$  is the total energy. Subsequently, we refer to the “ $B$  signal region,” which is defined as:

$$5.272 < M_{BC} < 5.289 \text{ GeV}/c^2; \quad |\Delta E| < 40 \text{ MeV}.$$

### III. BACKGROUND SUPPRESSION

To suppress the combinatorial background which is dominated by the two-jet-like  $e^+e^- \rightarrow q\bar{q}$  continuum process, we use variables that characterize the event topology. We require  $|\cos(\theta_{Thr})| < 0.80$  where  $\theta_{Thr}$  is the angle between the thrust axis of the  $B$  candidate and that of the rest of the event. This eliminates 83% of the continuum background and retains 79% of the signal events. Following the analysis of ref. [6], we define a Fisher discriminant  $\mathcal{F}$  that includes the angle of the thrust axis of the entire event, the production angle of the  $B$  meson candidate and nine “Virtual Calorimeter” [7] parameters that characterize the momentum flow in the event relative to the  $B$  candidate thrust axis. When the requirement on the Fisher discriminant variable  $\mathcal{F} > 0.5$  is imposed, 79% of the continuum background is rejected with about 74% efficiency for the signal. In the case of three charged kaon final states, the continuum background is much smaller and a looser requirement  $\mathcal{F} > 0$  can be imposed. This rejects 53% of the continuum background with about 89% efficiency for the signal.

In the  $K^+\pi^+\pi^-$  final state the background from  $B$  generic decays is dominated by the decays of type  $B^+ \rightarrow [K^+\pi^-]\pi^+$  where  $[K^+\pi^-]$  denotes a resonance state which can decay into  $K^+\pi^-$  such as  $D^0$ ,  $K^{*0}(892)$  etc. To suppress this type of background, we require the invariant mass of the  $K^+\pi^-$  system be greater than 2.0 GeV/ $c^2$ . For the  $K^+K^+K^-$  final state we require the invariant mass for both  $K^+K^-$  combinations be greater than 2.0 GeV/ $c^2$  to suppress the possible background from rare  $B$  decays such as  $B^+ \rightarrow \phi K^+$ .

## IV. RESULTS OF THE ANALYSIS

### A. Signal yield extraction

First, we select all  $K^+\pi^+\pi^-$  ( $K^+K^+K^-$ ) combinations from the  $B$  signal region that satisfy the selection criteria described above and have the  $\pi^+\pi^-$  ( $K^+K^-$ ) invariant mass in the range  $3.2 < M(h^+h^-) < 3.8$  GeV/ $c^2$ . The resulting  $\pi^+\pi^-$  and  $K^+K^-$  invariant mass spectra are shown in Figs. 1a and 1b, respectively. Since in the case of the  $K^+K^+K^-$  final state there are two same charge kaons, we distinguish the  $K^+K^-$  combination with the smaller,  $M(K^+K^-)_{min}$ , and larger,  $M(K^+K^-)_{max}$ , invariant masses. Only the larger combination is plotted. Two prominent peaks can be seen in Fig. 1a. The peak around 3.69 GeV/ $c^2$  corresponds to the  $\psi(2S)$  meson from the decay mode  $B^+ \rightarrow \psi(2S)K^+$ ,  $\psi(2S) \rightarrow \mu^+\mu^-$  with muons misidentified as pions. It is slightly shifted to higher mass values due to the wrong mass assignment for  $\psi(2S)$  daughter particles. The peak just above 3.4 GeV/ $c^2$  is identified as the  $\chi_{c0}$  meson.

The  $\pi^+\pi^-$  and  $K^+K^-$  spectra are fitted to the sum of a Breit-Wigner function convolved with a Gaussian for the signal and a zeroth-order polynomial for the background. The width of the Gaussian is fixed at 10.8 MeV/ $c^2$  as determined from a fit to the  $J/\psi$  peak in the  $\mu^+\mu^-$  invariant mass spectrum. The width of the Breit-Wigner function is fixed at the world average value for the  $\chi_{c0}$  [8]. The results of the fit to the  $\pi^+\pi^-$  and  $K^+K^-$  invariant mass spectra are given in Table I. The peak position in the  $K^+K^-$  spectrum, Fig. 1b, is found to be somewhat shifted to lower mass values. Although this shift is consistent with a statistical fluctuation, we note that according to the results of our general analysis of the three body  $B^+ \rightarrow K^+K^+K^-$  decay, we find a significant signal in the mass sidebands of the  $\chi_{c0} \rightarrow K^+K^-$  signal [6]. As a result, the  $K^+K^-$  invariant mass distribution in the  $\chi_{c0}$  region could be distorted by the effects of interference with an amplitude not related to the  $B^+ \rightarrow \chi_{c0}K^+$ . A Monte Carlo simulation study indicates that this effect could shift the  $\chi_{c0}$  peak position by as much as 15 MeV/ $c^2$  and could have as much as a 100% effect on the observed amplitude of the  $\chi_{c0}$  signal. Because of this uncertainty we base our branching fraction measurement for the  $B^+ \rightarrow \chi_{c0}K^+$  decay on the  $\chi_{c0} \rightarrow \pi^+\pi^-$  decay mode only.

TABLE I. Results of the fit to the  $\pi^+\pi^-$  and  $K^+K^-$  invariant mass spectra.

$\chi_{c0}$ submode	Efficiency, %	Peak, GeV/ $c^2$	Yield, events	Significance, $\sigma$
$\chi_{c0} \rightarrow \pi^+\pi^-$	21.5	$3.408 \pm 0.006$	$15.5^{+5.3}_{-4.6}$	4.8
$\chi_{c0} \rightarrow K^+K^-$	13.7	$3.390 \pm 0.009$	$7.7^{+3.9}_{-3.1}$	3.2

The  $\chi_{c0}$  candidates are then selected by requiring  $|M(h^+h^-) - 3.415| < 0.050$  GeV/ $c^2$ , where  $h^+h^-$  denotes both  $\pi^+\pi^-$  or  $K^+K^-$  combinations. This corresponds to about a 2.6  $\sigma$  cut. The resulting two-dimensional  $\Delta E$  versus  $M_{BC}$  plots as well as the projections on the  $\Delta E$  and  $M_{BC}$  axes are shown in Figs. 2 and 3 for the  $K^+\pi^+\pi^-$  and  $K^+K^+K^-$  final states, respectively. Clear signals are apparent in both figures.

## B. Branching fraction calculation

To determine branching fractions, we normalize our results to the observed  $B^+ \rightarrow \bar{D}^0\pi^+$ ,  $\bar{D}^0 \rightarrow K^+\pi^-$  signal. Although this introduces a 9.7% systematic error because of the uncertainty in the  $B^+ \rightarrow \bar{D}^0\pi^+$  branching fraction, it removes systematic effects in the particle identification efficiency, charged track reconstruction efficiency and the systematic uncertainty due to the cuts on event shape variables. We calculate the branching fraction for the  $B$  meson decay to a final state  $f$  via the relation:

$$\mathcal{B}(B \rightarrow f) = \mathcal{B}(B^+ \rightarrow \bar{D}^0\pi^+) \times \mathcal{B}(\bar{D}^0 \rightarrow K^+\pi^-) \frac{N_f}{N_{D\pi}} \times \frac{\varepsilon_{D\pi}}{\varepsilon_f}, \quad (1)$$

where  $N_f$  and  $N_{D\pi}$  are the numbers of observed events for the particular final state  $f$  and for the reference process respectively,  $\varepsilon_f$  and  $\varepsilon_{D\pi}$  are corresponding reconstruction efficiencies determined from the Monte Carlo simulation.

As a cross-check, we use the decay mode  $B^+ \rightarrow J/\psi K^+$  followed by the  $J/\psi \rightarrow \mu^+\mu^-$  decay. In this case there are two muons in the final state instead of two pions. To avoid additional systematic uncertainty in the muon identification efficiency, we do not use muon identification information for  $J/\psi$  reconstruction. Instead, we apply the same pion-kaon separation cut for muons from  $J/\psi$  as for pions from  $\chi_{c0}$ . The feed-down from the  $J/\psi \rightarrow e^+e^-$  submode is found to be negligible (less than 0.5%) after the application of the electron veto requirement.

The signal yields for the  $B^+ \rightarrow \bar{D}^0\pi^+$  and  $B^+ \rightarrow J/\psi K^+$  processes are extracted from fits to the  $\Delta E$  distributions shown in Fig. 4. The yields are found to be  $N_{D\pi} = 858 \pm 31$  and  $N_{J/\psi} = 323 \pm 19$  respectively. Using the corresponding reconstruction efficiencies of 23.5% and 29.4% we find the ratio,  $R$ , of branching fractions to be

$$R = \frac{\mathcal{B}(B^+ \rightarrow J/\psi K^+)}{\mathcal{B}(B^+ \rightarrow \bar{D}^0\pi^+)} = \frac{N_{J/\psi K}}{N_{D\pi}} \times \frac{\varepsilon_{D\pi}}{\varepsilon_{J/\psi K}} \times \frac{\mathcal{B}(\bar{D}^0 \rightarrow K^+\pi^-)}{\mathcal{B}(J/\psi \rightarrow \mu^+\mu^-)} = 0.196 \pm 0.014,$$

where only the statistical error is quoted. This result is in good agreement with the value calculated from PDG [8] data:  $0.189 \pm 0.026$ .

To calculate the branching fraction for the  $B^+ \rightarrow \chi_{c0}K^+$  decay mode, we use the signal yield determined from the fit to the  $h^+h^-$  invariant mass spectra to take into account the possible contribution from the non-resonant  $B^+ \rightarrow K^+h^+h^-$  decays that would produce signal-like distributions in both  $\Delta E$  and  $M_{BC}$ . Combining all the relevant numbers from Table I and the intermediate branching fractions from PDG [8], we find the branching fraction for the  $B^+ \rightarrow \chi_{c0}K^+$  decay mode to be:

$$\begin{aligned} \mathcal{B}(B^+ \rightarrow \chi_{c0}K^+) &= (8.0_{-2.4}^{+2.8} \pm 1.0 \pm 1.1) \times 10^{-4} \quad (\chi_{c0} \rightarrow \pi^+\pi^- \text{ mode}); \\ \mathcal{B}(B^+ \rightarrow \chi_{c0}K^+) &= (5.3_{-2.2}^{+2.7} \pm 0.7 \pm 0.8) \times 10^{-4} \quad (\chi_{c0} \rightarrow K^+K^- \text{ mode}), \end{aligned}$$

where the first error is statistical, the second is systematic, and the third is due to the uncertainty in the  $\chi_{c0} \rightarrow h^+h^-$  branching fractions. The systematic error consists of the uncertainty in the  $B^+ \rightarrow \bar{D}^0\pi^+$  and  $\bar{D}^0 \rightarrow K^+\pi^-$  branching fractions (9.7%), the uncertainty in the background parameterization in the fit to the  $h^+h^-$  spectra (7.8% for  $\pi^+\pi^-$  and 8.5% for  $K^+K^-$ ) and the uncertainty in the background and signal parameterization in the fit to

the  $\Delta E$  distribution for  $B^+ \rightarrow \bar{D}^0\pi^+$  signal (2.3%). As mentioned above, our qualitative estimates indicate that the model dependent error in the  $K^+K^+K^-$  final state could be very large. We do not present the quantitative estimation here because of the large uncertainty.

We also calculate the ratio of the branching fractions for the  $B^+ \rightarrow \chi_{c0}K^+$  and  $B^+ \rightarrow J/\psi K^+$  decays using only the  $\chi_{c0} \rightarrow \pi^+\pi^-$  submode:

$$\frac{\mathcal{B}(B^+ \rightarrow \chi_{c0}K^+)}{\mathcal{B}(B^+ \rightarrow J/\psi K^+)} = 0.77_{-0.23}^{+0.27} \pm 0.11,$$

where the first error is statistical and the second comes from the uncertainties in the  $J/\psi \rightarrow \mu^+\mu^-$  and  $\chi_{c0} \rightarrow \pi^+\pi^-$  branching fractions.

### C. Cross-check with $\chi_{c0} \rightarrow K^{*0}K^-\pi^+$ mode

As an additional cross-check, we reconstruct the  $\chi_{c0}$  meson in the multi-body  $K^+K^-\pi^+\pi^-$  final state. Although, in general, the branching fractions for  $\chi_{c0}$  decays to multi-body final states are significantly higher than those for  $\pi^+\pi^-$  and  $K^+K^-$ , these modes suffer from a much larger combinatorial background. This background is somewhat reduced in the  $K^+K^-\pi^+\pi^-$  final state because of the presence of two charged kaons. We further reduce the combinatorial background by requiring that at least one  $K\pi$  pair be consistent with  $K^*(892) \rightarrow K\pi$ :  $|M(K\pi) - 0.896| < 0.050 \text{ GeV}/c^2$ . We also use a tighter cut on the Fisher discriminant variable  $\mathcal{F} > 0.8$  to suppress the larger continuum background.

The resulting two-dimensional  $\Delta E$  versus  $M_{BC}$  plot as well as the  $\Delta E$  and  $M_{BC}$  projections are presented in Fig. 5. From the fit to the  $\Delta E$  distribution  $9.2_{-3.4}^{+3.9}$  signal events are found. Using the reconstruction efficiency of 7.2% from Monte Carlo, we obtain a branching fraction that is in agreement with that determined for the  $\pi^+\pi^-$  mode, namely

$$\mathcal{B}(B^+ \rightarrow \chi_{c0}K^+) = (7.0_{-2.6}^{+3.0} \pm 2.3) \times 10^{-4} \quad (\chi_{c0} \rightarrow K^{*0}K^-\pi^+ \text{ mode}),$$

where the first error is statistical and the second comes from the uncertainty in the  $\chi_{c0} \rightarrow K^{*0}K^-\pi^+$  branching fraction.

## V. CONCLUSION

We report the first observation of the  $B^+ \rightarrow \chi_{c0}K^+$  decay mode. The statistical significance of the signal is more than  $4\sigma$ . The preliminary branching fraction result is  $\mathcal{B}(B^+ \rightarrow \chi_{c0}K^+) = (8.0_{-2.4}^{+2.7} \pm 1.0 \pm 1.1) \times 10^{-4}$  which is comparable to that for the  $B^+ \rightarrow J/\psi K^+$  decay. This provides evidence for a significant nonfactorizable contribution in  $B$  to charmonium decay processes.

The branching fraction measured by Belle is slightly higher than the CLEO published upper limit. However, given the uncertainties on the result, it would be premature to claim that they disagree.



## ACKNOWLEDGEMENT

We wish to thank the KEKB accelerator group for the excellent operation of the KEKB accelerator. We acknowledge support from the Ministry of Education, Culture, Sports, Science, and Technology of Japan and the Japan Society for the Promotion of Science; the Australian Research Council and the Australian Department of Industry, Science and Resources; the Department of Science and Technology of India; the BK21 program of the Ministry of Education of Korea and the CHEP SRC program of the Korea Science and Engineering Foundation; the Polish State Committee for Scientific Research under contract No.2P03B 17017; the Ministry of Science and Technology of Russian Federation; the National Science Council and the Ministry of Education of Taiwan; the Japan-Taiwan Cooperative Program of the Interchange Association; and the U.S. Department of Energy.

## REFERENCES

- [1] G. Bodwin *et al.*, Phys. Rev. D **46**, 3703 (1992).
- [2] M. Beneke *et al.*, Phys. Rev. D **59**, 054003 (1999).
- [3] K.W. Edwards *et al.* (CLEO Collaboration), Phys. Rev. Lett. **86**, 30 (2001).
- [4] K. Abe *et al.* (Belle Collaboration), KEK Progress Report 2000-4 (2000), to be published in Nucl. Inst. and Meth. A.
- [5] KEKB B Factory Design Report, KEK Report 95-7 (1995), unpublished; Y. Funakoshi *et al.*, Proc. 2000 European Particle Accelerator Conference, Vienna (2000).
- [6] K. Abe *et al.* (Belle Collaboration), BELLE-CONF-0114; Submitted as a contribution paper to LP2001.
- [7] D.M. Asner *et al.* (CLEO Collaboration), Phys. Rev. D **53**, 1039 (1996).
- [8] D.E. Groom *et al.* (Particle Data Group), Eur. Phys. J. C **15**, 1 (2000).

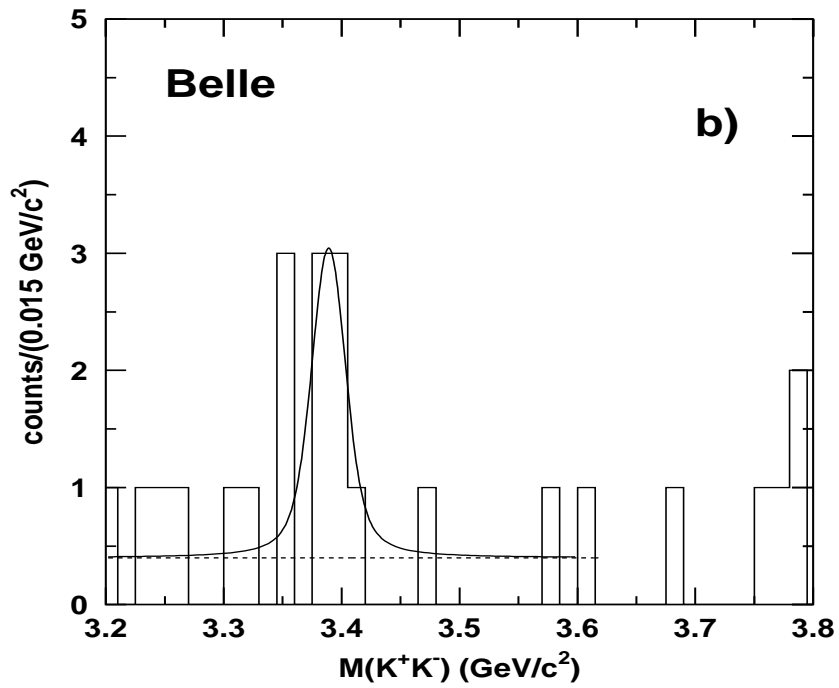
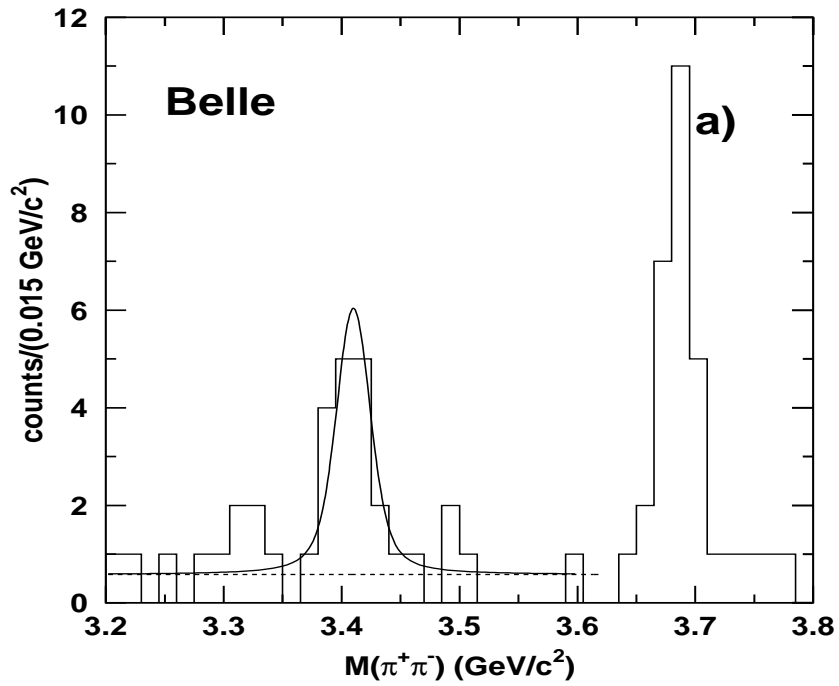


FIG. 1. The  $\pi^+\pi^-$  (a) and the  $K^+K^-$  (b) invariant mass spectra for  $B$  candidates from the signal region. The histograms are data and the curves are fits to the data.

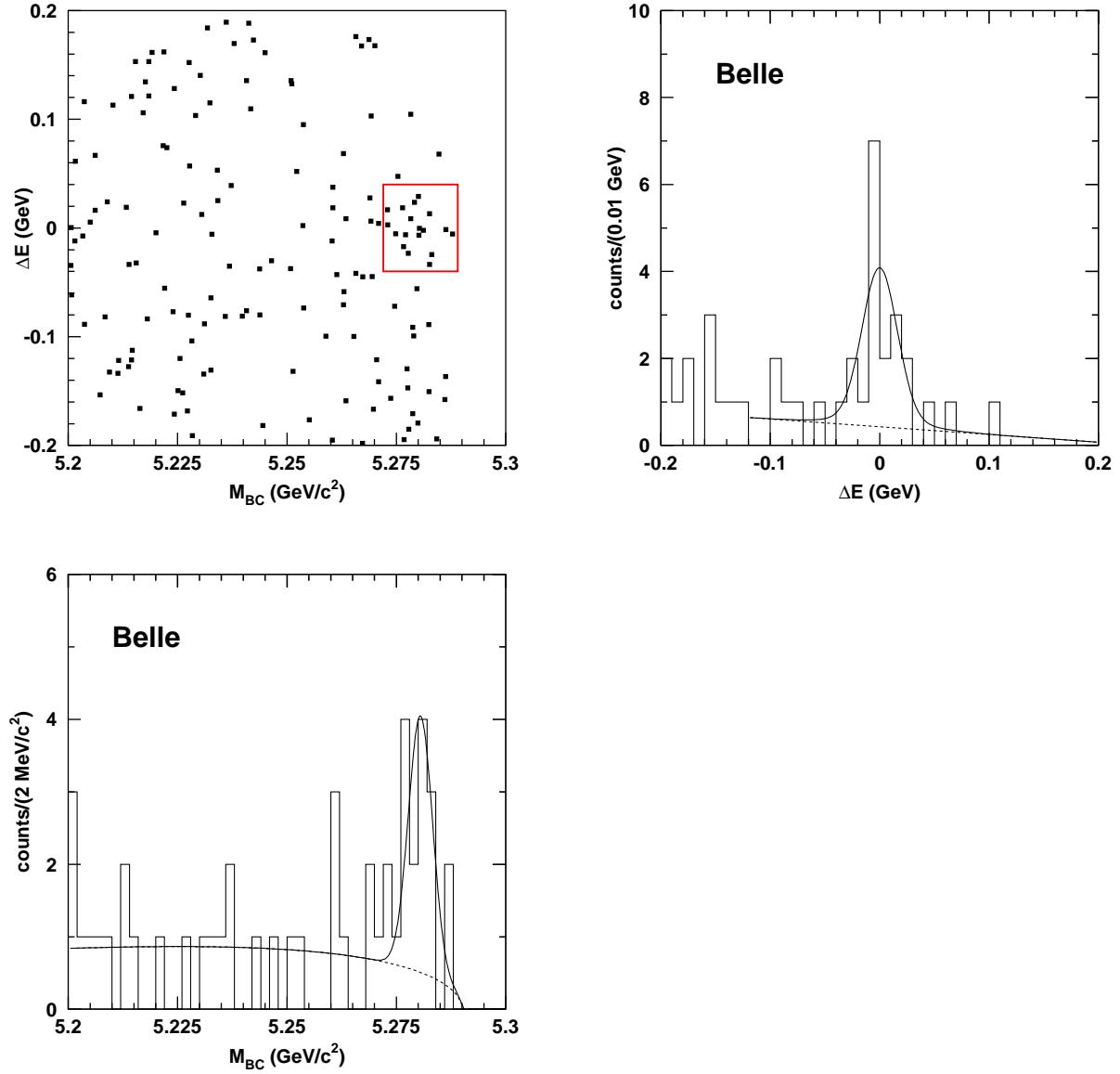


FIG. 2. The  $\Delta E$  and  $M_{bc}$  distributions for  $B^+ \rightarrow \chi_{c0} K^+$ ,  $\chi_{c0} \rightarrow \pi^+ \pi^-$  candidates. The box in the two-dimensional plot shows the signal region.

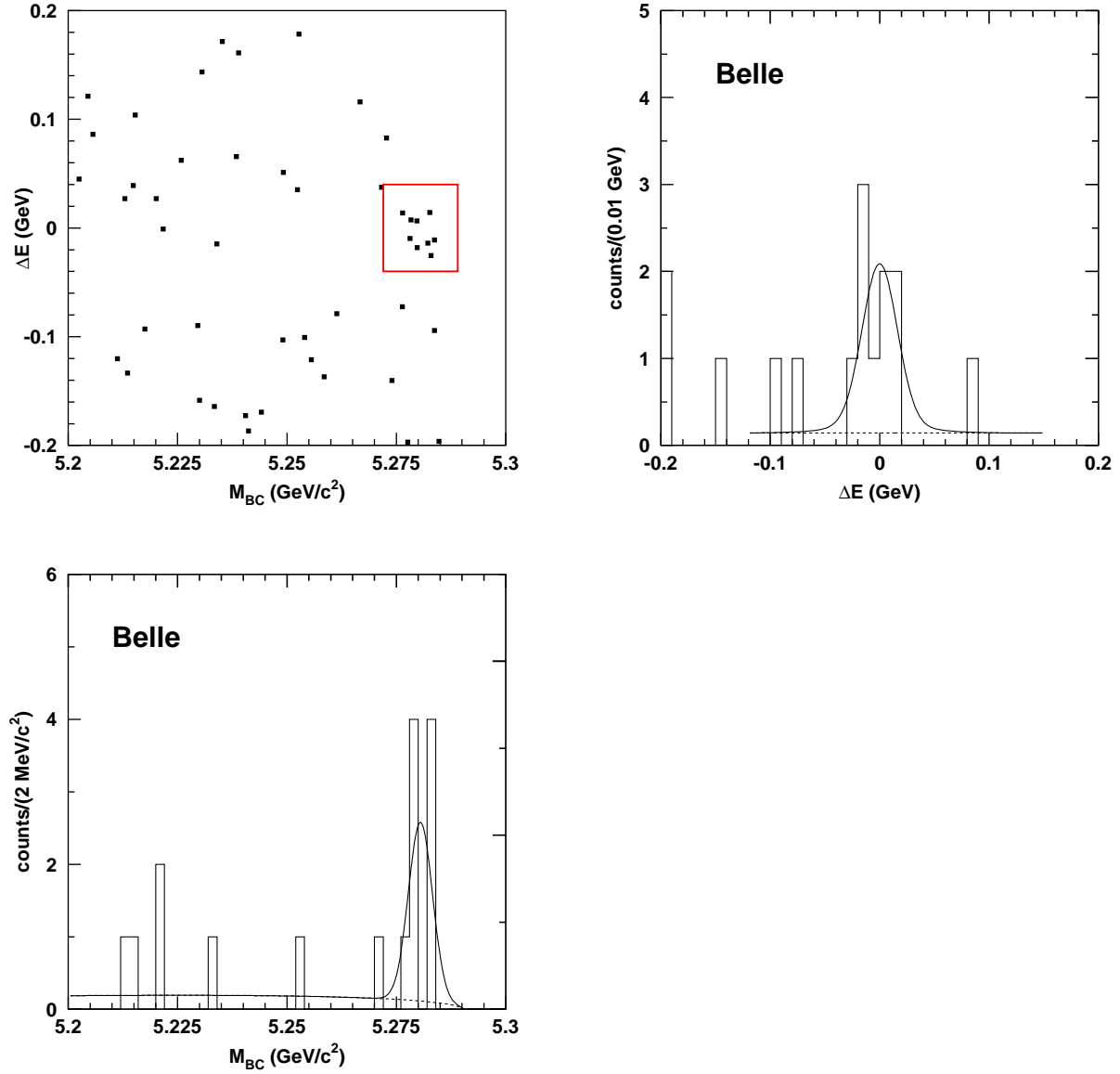


FIG. 3. The  $\Delta E$  and  $M_{bc}$  distributions for  $B^+ \rightarrow \chi_{c0} K^+$ ,  $\chi_{c0} \rightarrow K^+ K^-$  candidates. The box in the two-dimensional plot shows the signal region.

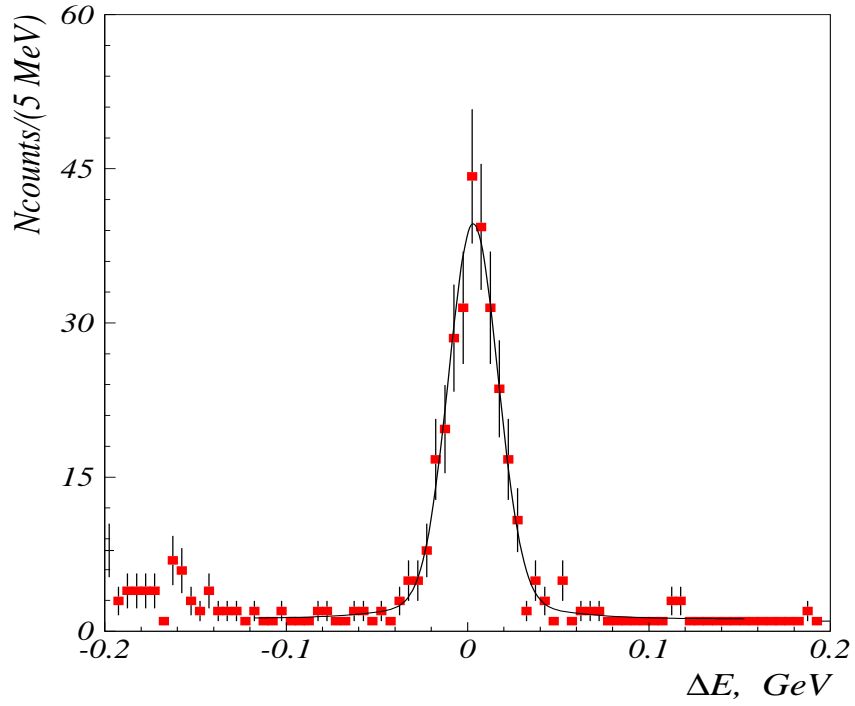
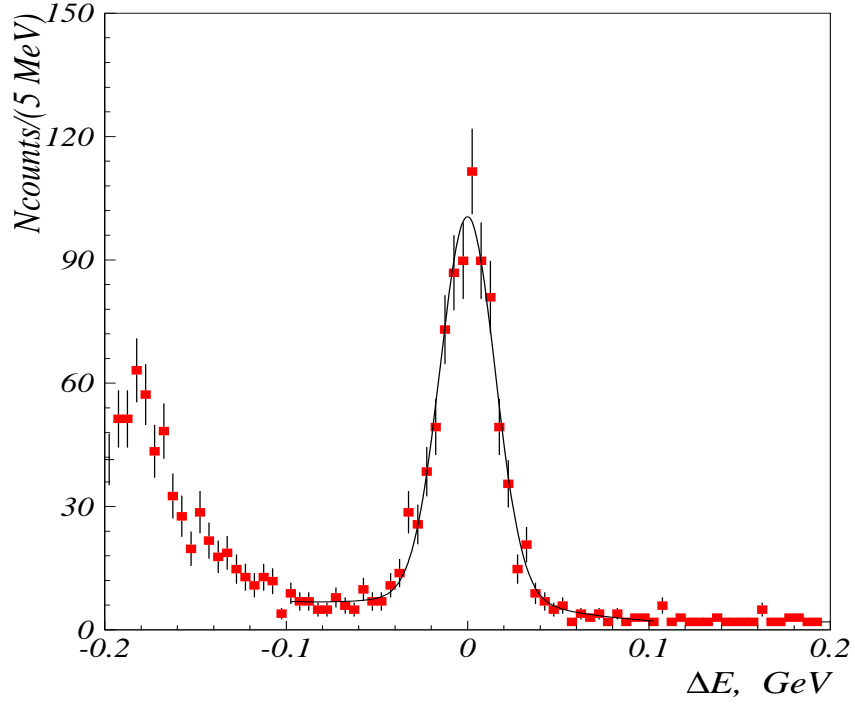


FIG. 4. The  $\Delta E$  distributions for reference processes: **a)** -  $B^+ \rightarrow \bar{D}^0\pi^+$ ,  $\bar{D}^0 \rightarrow K^+\pi^-$ ; **b)** -  $B^+ \rightarrow J/\psi K^+$ ,  $J/\psi \rightarrow \mu^+\mu^-$ .

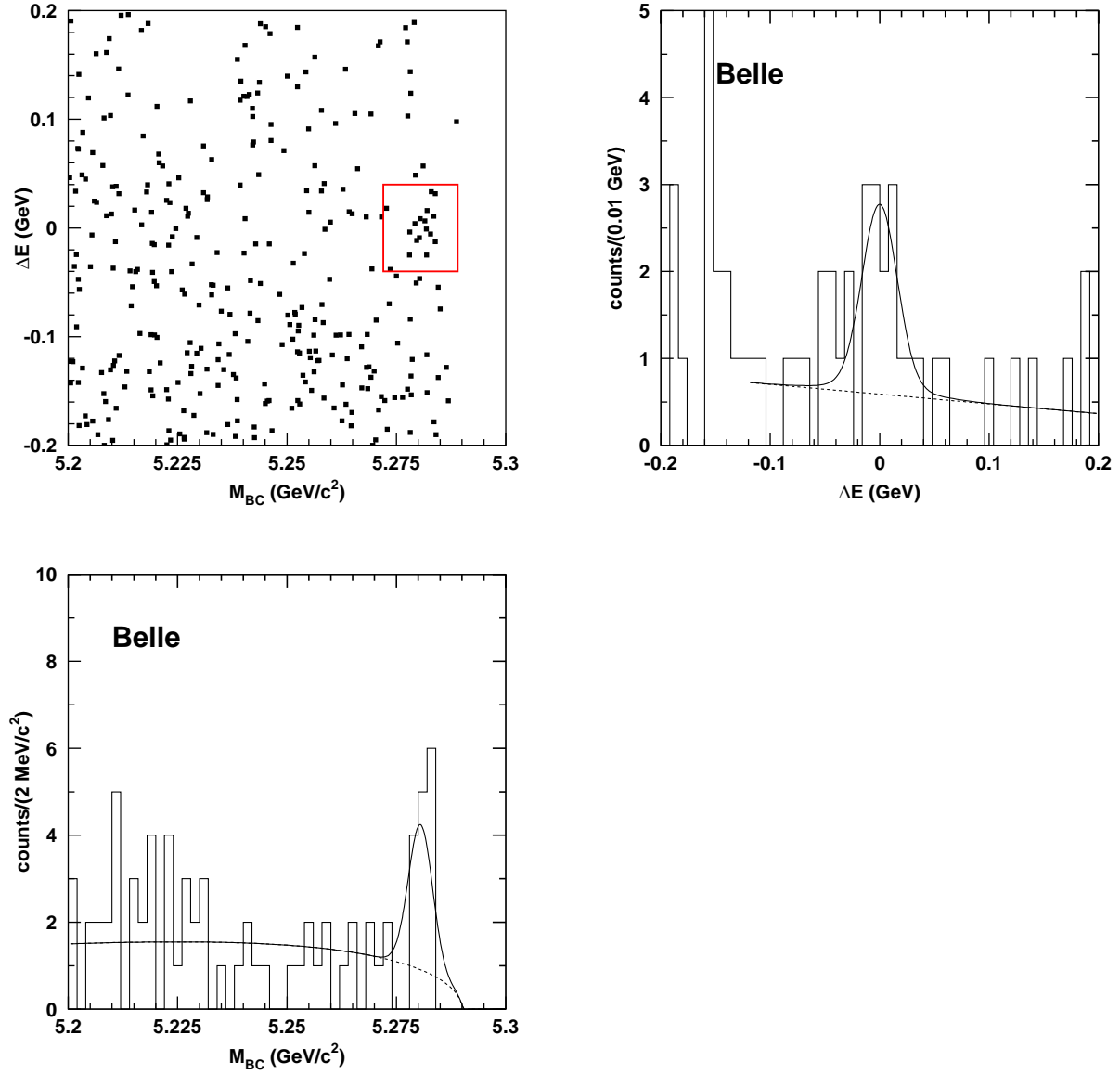


FIG. 5. The  $\Delta E$  and  $M_{bc}$  distributions for  $B^+ \rightarrow \chi_{c0} K^+$ ,  $\chi_{c0} \rightarrow K^{*0} K^+ \pi^-$  candidates. The box in the two dimensional plot shows the signal region.